Journal Name

COMMUNICATION

Self-Organization of Amino-Acid-Derived NDI Assemblies into a Nanofibrillar Superstructure with Humidity Sensitive *n*-Type Semiconducting Properties

Received 00th January 20xx,
Accepted 00th January 20xx

DOI: 10.1039/x0xx00000x

www.rsc.org/

Marco A. Squillaci,[‡a] Grzegorz Markiewicz,[‡b,c] Anna Walczak,[b,c] Artur Ciesielski,*[a] Artur R. Stefankiewicz,*[b,c] and Paolo Samorì*[a]

The hierarchical self-assembly of the L-tyrosine substituted naphtalenediimide has been explored in solution by NMR spectroscopy and in the solid-state by Atomic Force Microscopy. Spontanous non-covalent polymerisation led to the formation of a three-dimensional fibre-like supramolecular polymer with *n*-type semiconducting properties.

Suitably designed π-conjugated molecules can undergo spontaneous self-assembly forming spatially extended 1D (nanocolumns,[1] nanowires[2-3] or nanotubes[4-6]), 2D (nanosheets[7]) and 3D (3D-crystals[8]) supramolecular aggregates.[9-10] Such architectures hold unique physicochemical properties, which render them key components for various opto-electronic applications, including (photosensitive) field-effect transistors,[11-13] solar cells[14-15] and sensors.[16]

Among π-conjugated molecules, rylene dyes are widely studied *n*-type building blocks that combine high photochemical stability, high molar extinction coefficients and emission quantum yields, with ease of functionalization in different positions leading to a good solubility in organic solvents.[17-20] Naphthalenediimide (NDI) derivatives, small building blocks belonging to the rylene family, are air-stable *n*-type semiconductors well-known in organic electronics for their interesting electrical properties when aggregated in crystals.[8, 21] NDI can also be synthesized in the form of a co-polymer with dithiophene yielding high-mobility semiconducting polymers.[22] Achieving a full control on the molecular self-assembly at different length scales is of paramount importance in order to modulate the final properties of the material.[23-26]

It is well established that the functionalization of the imide nitrogen atoms of the NDI greatly affects the self-assembly behaviour and consequently the physical properties of the obtained materials such as their charge carrier mobility. In the specific case of NDI, the self-assembly is typically driven primarily by π-π stacking between the aromatic cores. By functionalizing the NDI cores with moieties capable of forming H-bonding, such as amino acids, it is possible to engineer a system which is prone to undergo self-assembly *via* two weak interactions, i.e. π-π stacking and H-bonding. When the molecule is properly designed, these two non-covalent forces can act simultaneously yet be in competition. In the last decade, Sanders and co-workers have pioneered the functionalization of NDIs with amino acids to create highly sophisticated supramolecular architectures. The use of S-trityl–L-cysteine units attached to the NDI led to the formation of helical supramolecular nanotubes held together primarily by H-bonding.[27] Conversely, when the NDI core is decorated with phenylalanine and unacylated tyrosine side chains π-π stacked polymers are generated, while the NDI functionalization with aliphatic L-isoleucine side chains yielded beta-sheet-like H-bonded supramolecular polymers.[28] The design of a system with balanced and tuneable strength of π-π stacking and H-bonding would represent a powerful tool to study the self-assembly in the solid-state, and selectively increase the strength of one of the two interactions type using an external remote control such as the relative humidity in the environment.

Here, we report the synthesis of a newly designed amino acid derived NDI (**1**) (Figure 1) that can undergo self-assembly forming fibrillar nanostructures as a result of the joint effect of two distinct non-covalent interactions, i.e. π-π stacking as well as O–H···O and C–H···O hydrogen bonds. Thanks to its unique chemical structure, it was possible to drive the self-assembly of **1** on a solid substrate towards a new type of 3D supramolecular polymer featuring a fibre-like motif. These supramolecular nanofibres show an air stable *n*-type semiconducting behaviour that is strongly influenced by atmospheric humidity. In particular, the increasing relative humidity in the environment yields a decrease of the strength

[a] *University of Strasbourg, CNRS, ISIS UMR 7006, 8 allée Gaspard Monge, F-67000 Strasbourg, France.*
[b] *Faculty of Chemistry, Adam Mickiewicz University, ul. Umultowska 89b, 61-614 Poznań, Poland.*
[c] *Center for Advanced Technologies, Adam Mickiewicz University, ul. Umultowska 89c, 61-614 Poznań, Poland.*
‡ These authors contributed equally to this work.
Electronic Supplementary Information (ESI) available: Supplementary NMR and AFM data, Dynamic Light Scattering, electrical characterization. See DOI: 10.1039/x0xx00000x

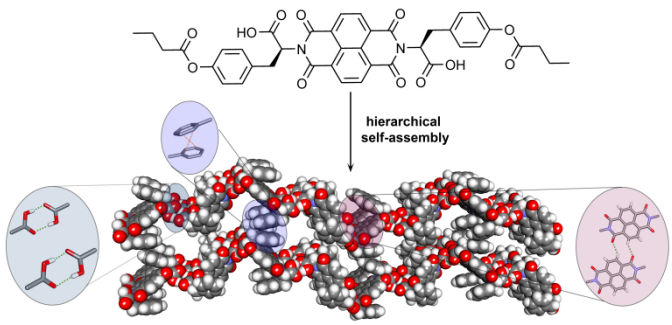

Figure 1. Hierarchical self-assembly of **1** into nanofibre-like architecture (C4 ester chains in 3D model were omitted for clarity).

of the H-bonding, leading to an increased overlap between the π orbitals of adjacent molecules within the aggregates thereby reducing the π-π stacking distance, that can be probed *via* electrical characterizations.[16, 29] The enantiomerically pure molecule **1** (Figure 1) was synthesized using a three-steps procedure, starting from commercial 1,4,5,8-naphthalenetetracarboxylic acid dianhydride (Figures S1-S8 ESI†). In order to obtain the desired supramolecular polymer, the molecular design comprises a flat, electron-deficient NDI core with two laterally located electron-rich tyrosine moieties exposing carboxylic acid groups capable of forming H-bonds. Acylation of the tyrosine hydroxyl groups was used both to enhance the solubility of the resulting supramolecular aggregates and to restrict H-bonding interactions only to those involving the carboxylic acid centres. The competition between π-π stacking and H-bonding interactions was expected to play a key role in the final self-assembly behaviour and to provide an adaptive nature to the supramolecular structure as a result of changes in the environmental conditions (choice of solvent or temperature). We found, that the interplay between three types of interactions, i.e. π-π stacking as well as H-bonding of COOH-HOOC and CH···O=C type, yielded the formation of fibrillar nanostructures whose motif is displayed in Figure 1.

The structure of the **1** based supramolecular polymer was studied by 1D and 2D NMR spectroscopy. Chloroform was employed as solvent because it has a relatively high polarity, it is a good solvent for **1** and it is a non-competitive medium for hydrogen bonds. The presence of intermolecular COOH-HOOC hydrogen bonding interactions between adjacent molecules was confirmed by comparing the ^{1}H NMR spectra recorded in $CDCl_3$ and DMSO-d_6 (Figure S9 in ESI†). The ^{1}H-NMR spectrum in $CDCl_3$ indicates the presence of a single symmetric conformation, fully consistent with the formation of an H-bonded structure, which is manifested by the broadening of the NMR resonance lines and deshielded signals of the α and β protons of the amino acid moiety. In contrast, the spectrum recorded in polar DMSO-d_6 exhibits sharp and shielded signals suggesting that H-bonding interactions have been disrupted. The formation of H-bonds was also demonstrated by simple protonation–deprotonation experiments. ^{1}H NMR studies carried out in chloroform, using triethylamine (Et_3N) and methanesulfonic acid (MSA) as base and acid respectively, was found to trigger the reversible switching between supramolecular polymer and monomeric structures in solution (Figures S 10-12 in ESI†). To determine whether the amino acid side chains adopt *syn* or *anti* geometry with respect to the NDI plane, ^{1}H-^{1}H Rotating frame Overhauser Effect Spectroscopy (ROESY) in $CDCl_3$ was performed (Figure 2). We identified ROE correlations between the NDI protons and tyrosine aromatic CH (couplings e, f) as well as the aliphatic α (coupling d) and C4 butyl chain hydrogens of the acyl-tyrosine units (couplings a, b, c), confirming that all of them are in close proximity to the NDI core. Only the aliphatic β protons of the amino acid did not display any ROE correlations with the NDI core (for detailed ROESY analysis see Table S1 in ESI†). The observed ROE correlations indicate, that the amino acid side-chains adopted an *anti*-geometry with respect to the NDI plane, as the alternative to *syn* conformation that would be sterically more hindered, leading to the loss of the ROE couplings between NDI core and tyrosine moieties and C4 butyl chains (couplings a, b, c, e, f). Such molecular morphology resembles this already reported by Iverson et al. for an NDI-based covalent polymer[30], in which the formation of an intramolecular π-π stacking is achieved using a flexible covalent linker between the aromatic cores.

To gain further insight into the molecular self-assembly in solution, ^{1}H NMR experiments in $CDCl_3$ were performed by varying the concentration (from 1×10^{-5} to 1×10^{-1} M) and the temperature (from 263 to 323 K). The single NDI resonance around 8.5 ppm of the **1** was found to be dependent on both factors (Figure S13 and 14 in ESI†), indicating the formation of higher order, hydrogen-bonded supramolecular assemblies in solution[31]. Variable temperature NMR experiments supported also the presence of the proposed additional C–H···O hydrogen bonds between the adjacent NDI components. Lowering the sample temperature leads to a gradual broadening of the NDI signal followed by splitting of the broad singlet into two peaks at 253 K, further resolved into two doublets at 243 K (Figure S15 in ESI†). Such features can be ascribed to the formation of well-defined and well-ordered hydrogen bonded architecture in which two different environments of the NDI aromatic protons are present leading to the splitting of their

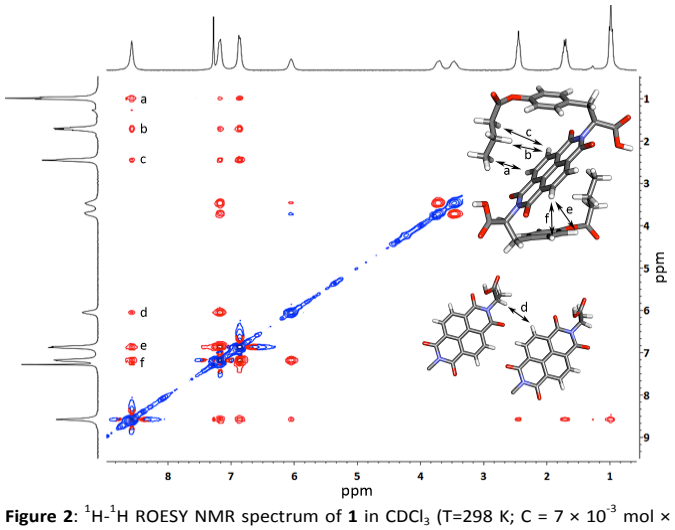

Figure 2: ^{1}H-^{1}H ROESY NMR spectrum of **1** in $CDCl_3$ (T=298 K; C = 7 × 10^{-3} mol ×

dm^{-3}) inset: 3D structures of **1** with assigned couplings (side chains and repetitive couplings were omitted for clarity).

^{1}H resonances. While these effects are quenched at room temperature by rather fast (on the NMR time scale) chemical exchange between NDI units, upon lowering the temperature the exchange is being slowed and the increase in the aggregation level is observed.

The particular conformation adopted by the molecule, with the two carboxylic groups pointing in opposite directions, determines its aggregation into high aspect ratio structures featuring a fibrillar shape. The growth of the assembly in $CHCl_3$ solution was confirmed by Dynamic Light Scattering (DLS) measurements (Figure S16 in ESI†) that provided evidence for a single distribution of species with an average size of 109.7 nm and a polydispersity of 0.44. To get a deeper insight into the morphology of the aggregates Atomic Force Microscopy (AFM) imaging was carried out on thin films prepared by drop casting of a solution of **1** in $CHCl_3$ (5 x 10^{-4} M) on SiO_2 substrates rendered hydrophobic through covalent functionalization with a monolayer of hexamethyldisilazane (HMDS) (Figure 3).

The AFM image shows that **1** forms tightly packed tubular structures exhibiting a rather uniform contrast along their contour. The supramolecular assemblies are structurally anisotropic: the fibres display a high aspect ratio, resulting from an average width of 43.3 nm and a length of several µm (Figure 3 and S17 in ESI†).

According to the proposed model in Figure 1 the fibrillar structures are stabilized by the simultaneous existence of H-bonding and π-π stacking between the phenyl rings of Tyr and the NDI core. The result of the intermolecular π-π stacking has a double effect: on the one hand it helps to stabilize the supramolecular structures, and on the other it gives arise to partially delocalized orbital between the molecule resulting in the appearance of electrical semiconducting properties typical for stacked π-conjugated systems.[32]

The electrical properties of the fibres-containing films have been characterized by integrating them in a bottom gate bottom contact field-effect transistor. The devices have been assembled by using SiO_2/Si substrates (oxide layer thickness 230 nm), baring pre-patterned interdigitated gold electrodes (channel length = 2.5 µm). The molecular films were obtained by employing the same procedure already described for the preparation of AFM samples. Such deposition results in a thin and uniform films of ordered fibres that are long enough to fully cover the whole channel, thereby bridging the source and drain electrodes (Figure S20 in ESI†).

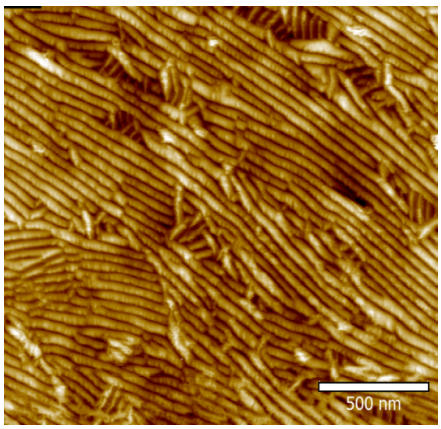

Figure 3. Topographical AFM images, recorded in intermittent contact mode, of film prepared by drop casting a solution of **1** on SiO_2 (Image Z-scale = 20 nm).

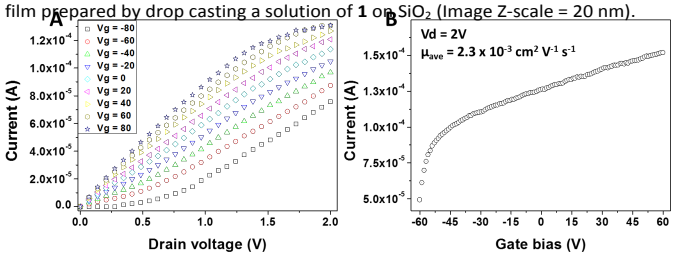

Figure 4. Output (A) and transfer (B) characteristic on fibres based films recorded in air.

Figure 4 displays the electrical output (A) and transfer (B) characteristics. The plots show an *n*-type semiconducting behaviour but, from the transfer characteristics in Figure 4B, it is also clear that there is a low current modulation by the gate and that the devices cannot be completely switched off by applying a negative gate bias (within the accessible range of gate biases). The average extracted n-type mobility measured for these devices amounts to 2.3*10^{-3} cm^2 V^{-1} s^{-1}; it is however noteworthy that all the electrical measurements reported in Figure 4 were performed in air, i.e. in an uncontrolled environment. Interestingly, when the same measurements are performed in controlled environment with extremely low levels of oxygen and water, no current, flowing through the fibers, can be detected under any condition of applied drain and gate biases.

The reason for this peculiar behaviour could be ascribed to from the presence of either oxygen or water in the environment. To understand which among these two components is playing the major role to enable efficient charge transport through the self-assembled films, new device characterizations recording I/V characteristics with a constant drain bias and pulsed flows of humid air or oxygen on the sample's surface were performed. While oxygen pulses did not give any modification in the drain current, pulses of humid air corresponded to a sharp increase in drain current, as displayed in Figure S21 in ESI†.

The reason for such behaviour can be ascribed to the structure of the self-assembled aggregates: the final structure is the result of a competition between H-bonding and π-π stacking. In a controlled atmosphere, such as in the N_2 filled glovebox, the strength of the H-bonding between molecules inside the fibres is very high and can easily overcome the contribution given from π-π stacking preventing a long-range intermolecular overlap between π orbitals. In a humid environment, water molecules absorbed from the atmosphere can disrupt the intermolecular H-bonding leaving the overlapping between π-orbitals as the major source of stabilization. This molecular rearrangement has, obviously, a strong impact on the mobility of charge carriers through the fibres based films.[16, 29]

In conclusion, we have synthesized a new NDI derivative that by design undergo self-assembly into fibre-like supramolecular polymers which are held together simultaneously by H-bonding and π-π stacking interactions. The co-existence of these two forces determines the morphology and properties of the supramolecular fibrillar structure. In particular, the presence of a tyrosine derivative as side chains in *anti*-geometry with respect to the NDI plane drives the aggregation into self-assembled fibers in which there is a degree of stacking of the tyrosine and NDI aromatic units. These supramolecular aggregates are markedly different from the ones already reported in literature for similar systems that, lacking tyrosine side chains, tend to self-assemble into chiral nanotubes not showing any π-π stacking and electrical properties.[31] In the present case, due to the nature and the structure of the aggregates, the fibrillar assemblies show the typical air stability and *n*-type semiconducting characteristics of NDI-based materials in which it is also possible to tune the electrical characteristics by modifying the humidity in the environment. The effect of humidity is so strong that the mobility increases from 0 to 10^{-3} cm^2 V^{-1} s^{-1} upon increasing the relative humidity from 0% to ambient conditions RH ~ 50%.

This work was financially supported by the National Centre for Research and Development (grant LIDER/024/391/L-5/13/NCBR/2014), Polish National Science Centre (Grant no. 2015/18/E/ST5/00188) and by EC through the Marie Sklodowska-Curie ITN project SYNCHRONICS (GA 643238), the Labex project CSC (ANR-10-LABX-0026 CSC) within the Investissement d'Avenir program ANR-10-IDEX-0002-02 and the International Center for Frontier Research in Chemistry (icFRC).

Notes and references

1. W. Pisula, A. Menon, M. Stepputat, I. Lieberwirth, U. Kolb, A. Tracz, H. Sirringhaus, T. Pakula and K. Müllen, *Adv. Mater.*, 2005, **17**, 684-689.
2. A. Schenning and E. W. Meijer, *Chem. Commun.*, 2005, 3245-3258.
3. P. Samorí, V. Francke, K. Müllen and J. P. Rabe, *Chem. Eur. J.*, 1999, **5**, 2312-2317.
4. J. P. Hill, W. Jin, A. Kosaka, T. Fukushima, H. Ichihara, T. Shimomura, K. Ito, T. Hashizume, N. Ishii and T. Aida, *Science*, 2004, **304**, 1481-1483.
5. C. Roeger, M. G. Müller, M. Lysetska, Y. Miloslavina, A. R. Holzwarth and F. Würthner, *J. Am. Chem. Soc.*, 2006, **128**, 6542-6543.
6. A. R. Stefankiewicz, E. Tamanini, G. D. Pantos and J. K. M. Sanders, *Angew. Chem. Int. Ed.*, 2011, **50**, 5724-5727.
7. B. Narayan, S. P. Senanayak, A. Jain, K. S. Narayan and S. J. George, *Adv. Funct. Mater.*, 2013, **23**, 3053-3060.
8. A. Lv, Y. Li, W. Yue, L. Jiang, H. Dong, G. Zhao, Q. Meng, W. Jiang, Y. He, Z. Li, Z. Wang and W. Hu, *Chem. Commun.*, 2012, **48**, 5154-5156.
9. L. Maggini and D. Bonifazi, *Chem. Soc. Rev.*, 2012, **41**, 211-241.
10. Z. Chen, A. Lohr, C. R. Saha-Moeller and F. Würthner, *Chem. Soc. Rev.*, 2009, **38**, 564-584.
11. S. Laschat, A. Baro, N. Steinke, F. Giesselmann, C. Haegele, G. Scalia, R. Judele, E. Kapatsina, S. Sauer, A. Schreivogel and M. Tosoni, *Angew. Chem. Int. Ed.*, 2007, **46**, 4832-4887.
12. F. Würthner and R. Schmidt, *Chemphyschem*, 2006, **7**, 793-797.
13. M. El Gemayel, M. Treier, C. Musumeci, C. Li, K. Müllen and P. Samorì, *J. Am. Chem. Soc.*, 2012, **134**, 2429-2433.
14. C. J. Brabec, N. S. Sariciftci and J. C. Hummelen, *Adv. Funct. Mater.*, 2001, **11**, 15-26.
15. L. Schmidt-Mende, A. Fechtenkotter, K. Mullen, E. Moons, R. H. Friend and J. D. MacKenzie, *Science*, 2001, **293**, 1119-1122.
16. M. A. Squillaci, L. Ferlauto, Y. Zagranyarski, S. Milita, K. Mullen and P. Samori, *Adv. Mater.*, 2015, **27**, 3170-3174.
17. T. Weil, T. Vosch, J. Hofkens, K. Peneva and K. Müllen, *Angew. Chem. Int. Ed.*, 2010, **49**, 9068-9093.
18. F. Würthner, C. R. Saha-Möller, B. Fimmel, S. Ogi, P. Leowanawat and D. Schmidt, *Chem. Rev.*, 2016, **116**, 962-1052.
19. J. E. Anthony, A. Facchetti, M. Heeney, S. R. Marder and X. Zhan, *Adv. Mater.*, 2010, **22**, 3876-3892.
20. N. Sakai, J. Mareda, E. Vauthey and S. Matile, *Chem. Commun.*, 2010, **46**, 4225-4237.
21. T. He, M. Stolte and F. Würthner, *Adv. Mater.*, 2013, **25**, 6951-6955.
22. H. Yan, Z. Chen, Y. Zheng, C. Newman, J. R. Quinn, F. Dötz, M. Kastler and A. Facchetti, *Nature*, 2009, **457**, 679-686.
23. V. Palermo and P. Samorì, *Angew. Chem. Int. Ed.*, 2007, **46**, 4428-4432.
24. S. Sergeyev, W. Pisula and Y. H. Geerts, *Chem. Soc. Rev.*, 2007, **36**, 1902-1929.
25. X. Zhan, A. Facchetti, S. Barlow, T. J. Marks, M. A. Ratner, M. R. Wasielewski and S. R. Marder, *Adv. Mater.*, 2011, **23**, 268-284.
26. S. Wang, M. Kappl, I. Liebewirth, M. Müller, K. Kirchhoff, W. Pisula and K. Müllen, *Adv. Mater.*, 2012, **24**, 417-420.
27. G. D. Pantos, P. Pengo and J. K. M. Sanders, *Angew. Chem. Int. Ed.*, 2007, **46**, 194-197.
28. N. Ponnuswamy, A. R. Stefankiewicz, J. K. M. Sanders and G. D. Pantoş, *Top. Curr. Chem.*, 2012, **322**, 217-260.
29. A. Bhattacharyya, M. K. Sanyal, U. Mogera, S. J. George, M. K. Mukhopadhyay, S. Maiti and G. U. Kulkarni, *Sci. Rep.*, 2017, **7**, 246-246.
30. R. S. Lokey and B. L. Iverson, *Nature*, 1995, **375**, 303-305.
31. N. Ponnuswamy, G. D. Pantos, M. M. Smulders and J. K. M. Sanders, *J. Am. Chem. Soc.*, 2012, **134**, 566-573.
32. V. Percec, M. Glodde, T. K. Bera, Y. Miura, I. Shiyanovskaya, K. D. Singer, V. S. K. Balagurusamy, P. A. Heiney, I. Schnell, A. Rapp, H. W. Spiess, S. D. Hudson and H. Duan, *Nature*, 2002, **417**, 384-387.

